Preparation of fluorescent carbon dots from peat for Fe^{3+} sensing and cellular imaging

Shuai Han[1,2], Baoshuang Wu[1], Hong Wang[3], Guangshuo Wang[1], Jiajia Yang[1], Leqin He[1], Fangfang Wei[1], Shenjun Qin[2] ✉

[1]*College of Materials Science and Engineering, Hebei University of Engineering, Handan, 056038, People's Republic of China*
[2]*Key Laboratory of Resource Exploration Research of Hebei Province, Hebei University of engineering, Handan, 056038, People's Republic of China*
[3]*First Department of Geriatrics, the first hospital of Hebei Shijiazhuang city, Shijiazhuang, 050011, People's Republic of China*
✉ *E-mail: qinsj528@hebeu.edu.cn*

Published in Micro & Nano Letters; Received on 13th May 2019; Revised on 5th September 2019; Accepted on 31st October 2019

Novel fluorescent carbon dots (CDs) were fabricated using the hydrothermal carbonisation method by peat, which is a very abundant and low-cost natural material in the world. The transmission electron microscopy images revealed that the peat-derived CDs (PCDs) are well-crystalline with an average size of 4 nm. Fourier transform infrared and X-ray photoelectron spectra suggested large amounts of oxygenous functionality which made the synthesised PCDs water-soluble. The optical characterisations turned out that PCDs showed a stable and excellent excitation-dependent photoluminescence (PL), while the quantum yield was calculated to be 18.3%. As the PL of the PCDs could be efficiently quenched by ferric ions with a low-detection limit of 20 nM, the as-prepared PCDs could be employed as a highly fluorescent probe for ferric ions. Furthermore, the obtained PCDs have been successfully used for fluorescent imaging and Fe^{3+} detecting at cell level.

1. Introduction: Fluorescent carbon dots (CDs), a superstar of the carbon nanomaterials in recent years, have attracted great attention owing to their unique physical and chemical properties, such as good modifiability, excellent photoluminescence (PL), low biological toxicity [1–3]. There are several methods for the preparation of CDs including laser ablation [4], microwave synthesis [5], chemical ablation, and hydrothermal/solvothermal treatment [6, 7]. However, these methods usually suffer from expensive precursors, low yield, and complex purification procedures [8]. As a result, major attention has been focused on green approach for the preparation of CDs using cheap precursors over the past decade [9, 10].

Fe^{3+}, one of the most common metal ions, plays various and important roles in the oxidation reaction, oxygen transport and other biological processes [11]. Mounting evidence suggests that neither deficiencies nor excesses of Fe^{3+} could trigger biology disorders for the human body, such as Huntington, Alzheimer's and Parkinson's disease [12]. Thus, the detection of Fe^{3+} is of great significance for early identification and diagnosis of these health problems. In recent years, many methods with good performance have been explored for selective and sensitive assay of Fe^{3+} [13]. However, there is still much room to develop new fluorescent sensors for Fe^{3+} with high sensitivity and selectivity.

Peat is a very abundant and low-cost natural material in the world, which is also considered to be a complex material with plant residues, humic acids, and minerals as major constituents [14]. Considering that the constituents are most of organic substances, such as lignin and humic acid, which have plenty of aromatic domains with alcohols, carboxylic acids and other polar functional groups [15], this inspired us to use peat as the carbon source to produce peat-derived CDs (PCDs). More importantly, it is further demonstrated that the obtained PCDs exhibit excellent PL sensitivity for Fe^{3+} detection and its potential applications in florescent imaging and Fe^{3+} monitoring in biosystem were explored.

2. Materials and experimental: The sphagnum peat was purchased from Pindstrup Industrial Group Co., Ltd (Denmark, model: 0–6 mm, pH = 4.5), while the chemical composition of the peat is shown in Table 1. Ammonia and other chemicals were obtained from Nanjing Chem. Reagent Co., Ltd (Nanjing, China). Distilled water was used throughout the experiments.

Transmission electron microscopy (TEM, JEOL-2010, Japan) measurements were operated at an accelerating voltage of 200 kV. The ultraviolet–visible (UV–vis) absorption spectrum was characterised by using an Agilent Cary 5000 spectrophotometer (USA). Fourier transform infrared (FTIR) spectra were recorded on a Nicolet 6700 FTIR spectrometer (USA) in the range of 4000–500 cm^{-1}. The composition of PCDs was determined using an X-ray photoelectron spectroscope (XPS, ESCALAB250, Thermo-VG Scientific Co., England) with monochromatic Al-K radiation (hn = 1486.6 eV). Fluorescent emission (EM) spectra of the as-synthesised PCDs were recorded on a Hitachi F-7000 fluorescence spectrophotometer (Japan). The quantum yield (QY) of the PCDs was determined at an excitation (EX) wavelength of 360 nm using quinine sulphate in 0.1 M sulphuric acid (QY = 0.54) as a standard [16].

PCDs were obtained by hydrothermal synthesis of sphagnum peat. In a typical synthesis, 1.5 g dried peat was dispersed in 60 ml H_2O and neutralised by diluted ammonia water. After that, the mixture was put into a 100 ml Teflon-lined stainless-steel autoclave, and hydro-thermally reacted at 180 °C for a period of 8 h. The obtained dark brown system was centrifuged for 12 min (rotational speed: 10,000 rpm) to separate the precipitate, and the solution was further dialysed in a dialysis bag (molecular weight cut-off = 4000) for 48 h. The PCDs were collected under vacuum freeze-drying conditions for further use (yield: ~31.5%).

In order to quantify the cytotoxicity of the obtained PCDs, 3-(4,5-Dimethylthiazol-2-yl)-2,5-diphenyltetrazolium bromide (MTT) colorimetric assay was arranged. HeLa cells were seeded in 96-well culture plates and cultured for 12 h in an incubator (37°C, 5% CO_2). Then the PCDs (concentrations: 0–300 μg ml^{-1}) in Dulbecco's modified Eagle's medium (DMEM) were transferred to each well. After 24 h incubation, MTT reagent (5 mg ml^{-1}, 30 μl) was added into each well. The culture medium was further removed after 4 h incubation of HeLa cells. Then, 150 μl of dimethyl sulphoxide was put into each well. The optical density

doi: 10.1049/mnl.2019.0314

Table 1 Chemical composition of sphagnum peat

	Organic matter	Coarse ash	Humic acid	Total N	P_2O_5	K_2O
content	96%	4%	42%	3.8%	0.5%	0.3%

of the mixture was determined at 490 nm using a microplate reader. Mean and standard deviation for the wells were also calculated and reported in [17].

For the cellular imaging experiments, HeLa cells were firstly seeded onto 35 mm glass bottom culture dishes. After incubation in DMEM with a humidified atmosphere containing 5% CO_2 at 37°C for 24 h, the cells were treated with 20 μM PCDs for 12 h and washed three times with phosphate-buffered saline (PBS). The fluorescence imaging of the treated cells was observed under 370 nm EX (Olympus FV1000 confocal microscope, Tokyo, Japan; 40× objective lens). For assessing Fe^{3+} uptake, HeLa cells were incubated with 20 μM PCDs for 12 h at the same culturing conditions, followed by treated by 2 mM $Fe(NO_3)_3$ as the fluorescence quenching agent for another 0.5 h.

3. Results and conclusion: The morphology and size of the PCDs were identified by TEM (Fig. 1*a*). It could be observed that the obtained PCDs are mostly of spherical morphology (diameter: 2–5 nm) and disperse rather evenly. As further shown in Fig. 1*b*, most of the PCDs observed to be carbon particles with lattice fringes of 0.32 nm, corresponding to the ⟨002⟩ spacing of graphitic (sp^2) carbon [18].

The FTIR spectra of PCDs are shown in Fig. 2. The broad absorption peak in the region of 3200–3700 cm^{-1} could be associated with stretching vibrations of O–H and N–H. The emerging peaks at 2920 and 2850 cm^{-1} arouse from the stretching of C–H bonds [19]. The peak at 1650 cm^{-1} could be associated with the stretching vibrations of C=O. The absorption peaks at 1420 and 1570 cm^{-1} could be attributed to the stretching vibrations of C=C and the bending of N–H, respectively [20].

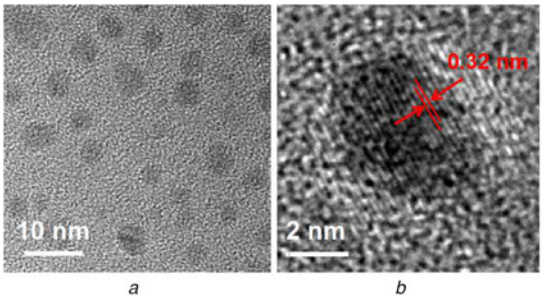

Fig. 1 *TEM images of the PCDs*
a TEM image
b High-resolution TEM image of the PCDs

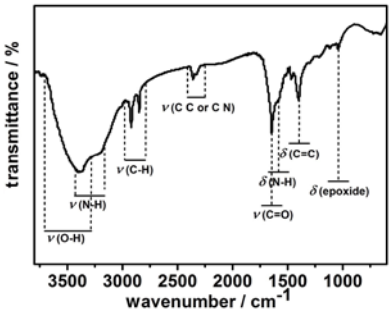

Fig. 2 *FTIR spectra analysis of the PCDs*

XPS measurement was explored to gain further insight into the chemical composition and functional groups of the PCDs. As shown in Fig. 3*a*, the full scan XPS spectra revealed that the PCDs were mainly composed of C (74.80%), N (5.50%), O (18.70%) and S (1.0%). The C 1s XPS spectrum in Fig. 3*b* exhibited four types of carbon atoms: graphitic or aliphatic (sp^2 C=C and C–C), C=O or C=N, oxygenated and nitrous [21]. The XPS results reveal that the obtained PCDs are functioned by plenty of groups with oxygen, nitrogen and sulphur elements, which is in good agreement with the results obtained from FTIR analysis.

The optical properties of the PCDs in aqueous solution were further explored. The UV–vis spectrum of the obtained PCDs (Fig. 4*a*) reveals a strong absorption peak focused on 315 nm, which could be ascribed to π–π* transition of C=C aromatic bonds [22]. Furthermore, the EX wavelength-dependent fluorescence behaviour was also found (Fig. 4*b*) [23, 24], while the strongest EM spectrum occurred at the EX wavelength of 389 nm. This behaviour might be caused by the different sizes and surface defects of the obtained PCDs. The QY of the obtained PCDs was calculated to be about 18.3% when the EX wavelength was fixed at 389 nm, demonstrating excellent fluorescent properties.

Typically, the functional groups on the surfaces of the CDs could contribute to strong coordination with metal ions. This strong interaction supplies the possibility of using the PCDs as a fluorescent sensor for cation detection [25]. The fluorescence of the PCDs could be efficiently quenched by Fe^{3+} ions. With the increasing of Fe^{3+} concentration, from 2 to 250 μM, the PL intensity gradually decreased to 20% of its initial value as shown in Fig. 5. Fig. 6 shows the dependence of $(F–F_0)/F_0$ on the concentration of Fe^{3+} ions, where F_0 and F are the PL intensities at 442 nm in the absence and presence of Fe^{3+}, respectively [26]. Interestingly, the $(F–F_0)/F$ curve shows a linear dependence on the Fe^{3+} concentration in the range of 5–120 μM, indicating the good sensing properties of PCDs in the monitoring of Fe^{3+}. It is worthy to mention that the fluorescence of the PCDs could the efficiently

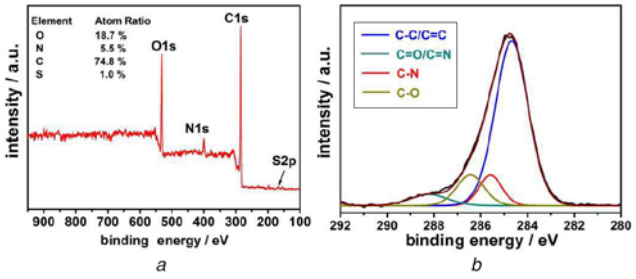

Fig. 3 *XPS of the PCDs*
a XPS spectrum
b High-resolution C 1s spectra analysis of the PCDs

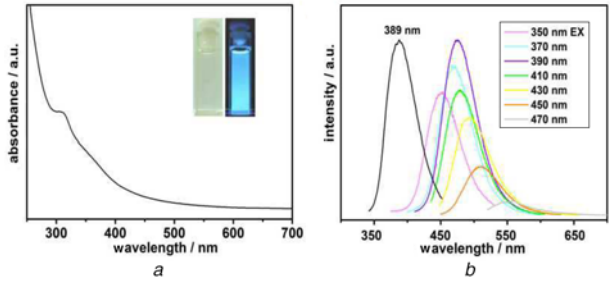

Fig. 4 *Optical analysis results of the PCDs in aqueous solution*
a UV–vis absorption spectra
b EX-dependent photoluminescence spectra of PCDs; the EX spectra were monitored at the maximum EM peak of 435 nm (black line)

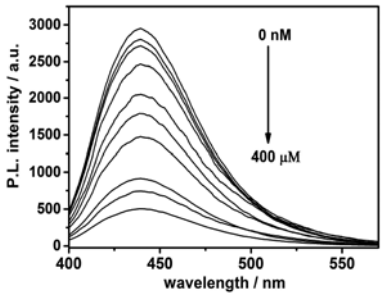

Fig. 5 *Fluorescence responses of the PCDs in aqueous solution with different concentrations of ferric ions (from top to bottom: 0, 3, 8, 25, 50, 70, 120, 180, 250,400 μM, respectively)*

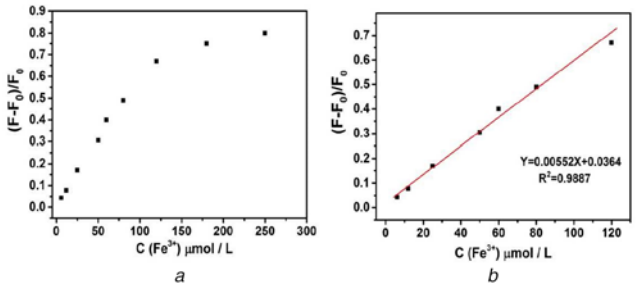

Fig. 6 *Dependence of (F_0–F)/F_0 on the concentration of Fe^{3+} ions*
a Dependence of $(F–F_0)/F_0$ on the concentration of ferric ions within the range of 2–250 μM
b Plot of the fluorescent response $(F–F_0)/F_0$ versus the logarithm of concentrations of ferric ions

quenched with a detection limit as low as 20 nM calculated from the plot of the fluorescent response $(F_0–F)/F_0$, which was found to be much lower than that of the previously reported carbon nanomaterials [27].

The PL quenching effect of various metal ions on PCDs was further researched. Different ions such as Na^+, K^+, Mg^{2+}, Al^{3+}, Ca^{2+}, Cr^{3+}, Fe^{2+}, Co^{2+}, Cu^{2+}, Zn^{2+}, Ag^+, Hg^{2+}, Pb^{2+} and Fe^{3+} with the same concentration of 1 mM, were added to PCDs solution (0.10 mg ml^{-1}) and reacted. Notably, it is shown in Fig. 7 the presence of different metal ions would lead to slight PL changes in the PL intensity (defined as the retention of fluorescence intensity more than 70% as compared to blank), however, as compared with other cations, Fe^{3+} shows the most obvious quenching effect on the PL intensity with the lowest F/F_0 value of −0.03. Such a specific PL quenching effect might be caused by strong coordination between ferric ions and the surface groups of PCDs [28]. In general, the high sensitivity together with the excellent selectivity for Fe^{3+} makes the PCDs a promising PL platform for the detection of Fe^{3+}.

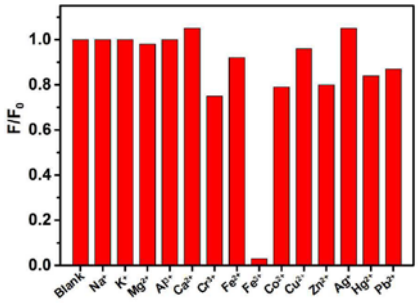

Fig. 7 *Relative change in fluorescence intensity of PCDs (0.10 mg ml^{-1}) after reacting with different metal ions (1 mM)*

In order to explore the practical application value, the stability of the PCDs was further studied. The PCDs showed excellent photostability, while the PL intensity of PCDs was almost unchanged under continuous irradiation (365 nm) for 60 min with a Xe lamp. It is shown in Fig. 8*b* that PCDs exhibit pH-dependent PL properties: the PL intensity reaches the highest at neutrality and obviously decreases under both strongly acidic

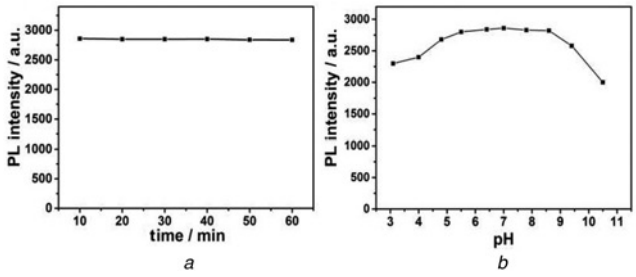

Fig. 8 *Fluorescence intensity variation of the PCDs as a function of*
a Irradiation time
b pH

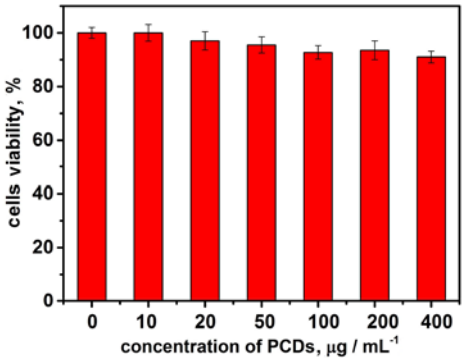

Fig. 9 *MTT assay for cell viability after incubation with concentrations series of PCDs for 36 h*

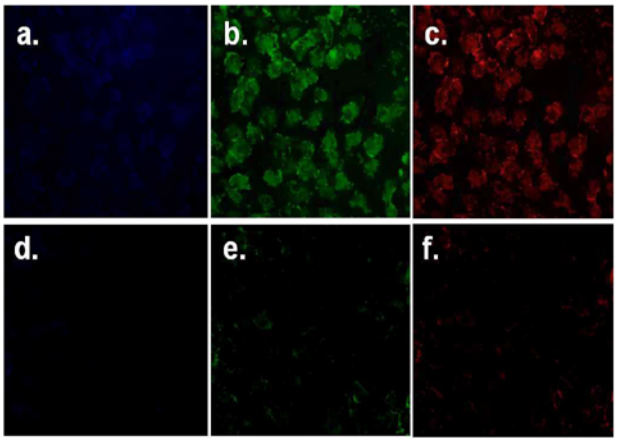

Fig. 10 *Photographs obtained from the confocal microscopy experiments*
a Confocal fluorescence digital photographs of HeLa cells after incubation with the PCDs (0.2 mg ml^{-1}): images were obtained at EX wavelengths of 365 nm
b 458 nm
c 546 nm
d Followed by further incubation with Fe^{3+}(2 mM), at EX wavelengths of 365 nm
e 458 nm
f 546 nm

doi: 10.1049/mnl.2019.0314

and basic conditions. This phenomenon might be caused by protonation−deprotonation of the surface functional groups [29]. It is worthy to mention that the PL intensity remains almost constant under the condition of pH = 5.2–8.5, which might help the PCDs to be a stable fluorescent probe in physiological conditions.

The MTT colourimetric assay was further carried out on HeLa cells before application to evaluate the cytotoxicity of the PCDs. It is shown in Fig. 9 that the obtained PCDs exhibit small toxicity towards HeLa cells even at high concentrations (400 μM) with long incubation times (36 h). Therefore, they are considered to be safe and suitable in bioimaging and other biomedical applications [30].

Confocal microscopy experiments were conducted to explore the applications of the PCDs as a nanosensor for the determination of Fe^{3+} ions in living cells. After incubation with PCDs in PBS for 8 h at 37°C, HeLa cells exhibited strong intracellular fluorescence, which was mainly localised in the perinuclear area of the cytoplasm. The EX wavelength-dependent fluorescence behaviour was further observed, the cell internalised CDs can be excited by laser irradiation at 365, 458, and 546 nm, and emitted blue, green, and red fluorescence (Figs. 10*a*, *b*, and *c*). Followed by adding 2 mM Fe^{3+} for 0.5 h, however, the intracellular fluorescence was seriously induced (Figs.10*d*, *e*, and *f*). All the biological results established that PCDs can be an effective probe for the detection of Fe^{3+} ions in biosystem [31].

4. Conclusion: In conclusion, novel PCDs were fabricated using the hydrothermal method by peat for the first time. The as-prepared PCDs showed a clear lattice structure with a narrow size distribution (3–5 nm) and exhibited excellent PL properties with a QY of 18.2%. Moreover, PCDs could serve as a PL probe for the highly sensitive and selective detection of ferric ion. It is shown from the MTT assay and cellular experiment that the PCDs have low cytotoxicity, and successfully applied as a nano-sensor for monitoring Fe^{3+} in cells. Combining its green synthetic route, excellent PL properties, and favourable biocompatibility, it is anticipated that the PCDs could be potential nano-agents in biological applications.

5. Acknowledgments: This work was supported by the Natural Science Foundation of Hebei Province of China (grant nos E2018402211, D2018402093, and B2016402081), and the Foundation of Hebei Educational Committee (grant nos QN2018008 and ZD2019055).

6 References

[1] Kumar A., Chowdhuri A., Laha D., *ET AL.*: 'Green synthesis of carbon dots from Ocimum sanctum for effective fluorescent sensing of Pb^{2+} ions and live cell imaging', *Sensor. Actuat. B, Chem.*, 2017, **242**, pp. 242–675

[2] Cheng Q., He Y., Ge Y., *ET AL.*: 'Dual-detection-window fluorescence probe for ultra-sensitive determination of Pb^{2+} based on emission-tunable B and N co-doped carbon dots'. *Micro Nano Lett.*, 2018, **13**, pp. 1175–1178

[3] Zhu C., Fu Y., Liu C., *ET AL.*: 'Carbon dots as fillers including healing/self-healing and anticorrosion properties in polymers', *Adv. Mater.*, 2017, **29**, pp. 1701399–1701407

[4] Calabro R., Yang D., Kim D., *ET AL.*: 'Liquid-phase laser ablation synthesis of graphene quantum dots from carbon nano-onions: comparison with chemical oxidation', *J. Colloid Interface Sci.*, 2018, **527**, pp. 132–140

[5] Hinterberger V., Wang W., Damm C., *ET AL.*: 'Microwave-assisted one-step synthesis of white light-emitting carbon dot suspensions', *Opt. Mater.*, 2018, **80**, pp. 110–119

[6] Calabro R., Yang D., Kim D.: 'Liquid-phase laser ablation synthesis of graphene quantum dots from carbon nano-onions: comparison with chemical oxidation', *J. Colloid Interface Sci.*, 2018, **527**, pp. 132–140

[7] Zhang J., Wang J., Fu X., *ET AL.*: 'Rapid synthesis of N,S co-doped carbon dots and their application for Fe^{3+} ion detection', *J. Nanopart. Res.*, 2018, **20**, p. 41

[8] Zhang J., Yu S.: 'Carbon dots: large-scale synthesis, sensing and bioimaging', *Mater. Today*, 2016, **19**, pp. 382–393

[9] Han S., Zhang H., Kang L., *ET AL.*: 'A convenient ultraviolet irradiation technique for synthesis of antibacterial Ag–Pal nanocomposite', *Nanoscale Res. Lett.*, 2016, **11**, pp. 431–437

[10] Emam A., Mohamed M., Gadall ah A., *ET AL.*: 'Enhancement of the collective optical properties of plasmonic hybrid carbon dots via localized surface plasmon', *J. Lumin.*, 2018, **200**, pp. 287–297

[11] Song Y., Zhu C., Song J., *ET AL.*: 'Drug-derived bright and color tunable N-doped carbon dots for cell imaging and sensitive detection of Fe^{3+} in living cells'. *ACS Appl. Mater. Interfaces*, 2017, **9**, pp. 7399–7405

[12] Ge G., Jiang Y., Jia H., *ET AL.*: 'On–off–on fluorescent nanosensor for Fe^{3+} detection and cancer/normal cell differentiation via silicon-doped carbon quantum dots', *Carbon*, 2018, **134**, pp. 232–243

[13] Vadivel R., Subray S., Ramamurthy P.: 'A green synthesis of highly luminescent carbon dots from itaconic acid and its application as an efficient sensor for Fe^{3+} ions in aqueous medium'. *New J. Chem.*, 2018, **42**, pp. 8933–8942

[14] Panneer S., Lapierre J., Guillemette F., *ET AL.*: 'Degradation potentials of dissolved organic carbon (DOC) from thawed permafrost peat', *Sci. Rep.*, 2017, **7**, pp. 45811–45820

[15] Dong L., Zhang W, Li X., *ET AL.*: 'Preparation of CQDs with hydroxyl function for Fe^{3+} detection', *Micro Nano Lett.*, 2019, **14**, pp. 440–444

[16] Wang Z., Xu C., Lu Y., *ET AL.*: 'Visualization of adsorption: luminescent mesoporous silica-carbon dots composite for rapid and selective removal of U(VI) and in-situ monitoring the adsorption behavior', *ACS Appl. Mater. Interfaces*, 2017, **9**, pp. 7392–7398

[17] Reid P., Wilson P., Li Y., *ET AL.*: 'Experimental investigation of radiobiology in head and neck cancer cell lines as a function of HPV status, by MTT assay', *Sci. Rep.*, 2018, **8**, pp. 7744–7750

[18] Han S., Zhang H., Xie Y., *ET AL.*: 'Application of cow milk-derived carbon dots/AgNPs composite as the antibacterial agent', *Appl. Surf. Sci.*, 2015, **328**, pp. 368–373

[19] Zhang Y., Foster C., Banks C., *ET AL.*: 'Graphene-rich wrapped petal-like rutile TiO_2 tuned by carbon dots for high-performance sodium storage', *Adv. Mater.*, 2016, **18**, pp. 9391–9399

[20] Zhou Y., Benetti D., Tong X., *ET AL.*: 'Colloidal carbon dots based highly stable luminescent solar concentrators', *NanoEnergy*, 2018, **44**, pp. 378–387

[21] Stan C., Horlescu P., Ursu L., *ET AL.*: 'Facile preparation of highly luminescent composites by polymer embedding of carbon dots derived from *N*-hydroxyphthalimide', *J. Mater. Sci.*, 2017, **52**, pp. 185–196

[22] Kumar A., Chowdhuri A., Laha D., *ET AL.*: 'Green synthesis of carbon dots from Ocimum sanctum for effective fluorescent sensing of Pb^{2+} ions and live cell imaging', *Sensor. Actuat. B, Chem.*, 2017, **242**, pp. 679–686

[23] Alas M., Gencb R.: 'An investigation into the role of macromolecules of different polarity as passivating agent on the physical, chemical and structural properties of fluorescent carbon nanodots', *J. Nanopart. Res.*, 2017, **19**, pp. 185–199

[24] Mixo X., Qu D., Yang D., *ET AL.*: 'Photoluminescence: synthesis of carbon dots with multiple color emission by controlled graphitization and surface functionalization', *Adv. Mater.*, 2017, **30**, pp. 1870002–1870010

[25] Jing N., Tian M., Wang Y., *ET AL.*: 'Nitrogen-doped carbon dots synthesize *d* from acrylic acid and ethylenediamine for simple and selective determination of cobalt ions in aqueous media', *J. Lumin.*, 2019, **206**, pp. 169–175

[26] Aslandas A., Balci N., Arik M., *ET AL.*: 'Liquid nitrogen-assisted synthesis of fluorescent carbon dots from Blueberry and their performance in Fe^{3+} detection', *Appl. Surf. Sci.*, 2015, **356**, pp. 747–752

[27] Vadivel R., Subray S., Ramamurthy P.: 'A green synthesis of highly luminescent carbon dots from itaconic acid and its application as an efficient sensor for Fe^{3+} ions in aqueous medium', *New J. Chem.*, 2018, **42**, pp. 8933–8942

[28] Chandra S., Chowdhuri A., Laha D., *ET AL.*: 'Fabrication of nitrogen and phosphorous-doped carbon dots by the pyrolysis method for iodide and iron(III) sensing', *Luminescence*, 2017, **33**, pp. 336–344

[29] Kang M., Singh R., Kim T., *ET AL.*: 'Optical imaging and anticancer chemotherapy through carbon dot created hollow mesoporous silica nanoparticles', *Acta Biomater.*, 2017, **55**, pp. 466–480

[30] Liao J., Cheng Z., Zhou L.: 'Nitrogen-doping enhanced fluorescent carbon dots: green synthesis and their applications for bioimaging and label-free detection of Au^{3+} ions', *ACS Sustain. Chem. Eng.*, 2016, **4**, pp. 3053–3061

[31] Hu S., Qiao S., Xu B., *ET AL.*: 'Dual-functional carbon dots pattern on paper chips for Fe^{3+} and ferritin analysis in whole blood', *Anal. Chem.*, 2017, **89**, pp. 2131–2137